# *PERTURBATION OF A MAGNETIC FIELD BY PLASMA OF A LASER SPARK IN AIR*

M. M. SAVCHENKO and V. K. STEPANOV

P. N. Lebedev Physics Institute, Academy of Sciences, U.S.S.R.

Submitted to JETP editor July 11, 1966

J. Exptl. Theoret. Phys. (U.S.S.R.) 51, 1654—1659 (December, 1966)

The results of a detailed study of a diamagnetic perturbation of an external magnetic field by plasma from a laser-induced spark in air are presented. It is shown that the perturbing region is small in comparison with the luminous region. The perturbation has a long duration, with a lifetime of 30—40 $\mu$, but the presence of a shock wave reflected from the obstacles near the spark reduces the lifetime and causes a conversion from diamagnetic to paramagnetic perturbation.

EARLIER experiments[1] showed that the plasma of a laser-induced spark in air forces the external magnetic field out of the measuring coil around the spark for a protracted period of time. The present paper reports some results of a further study of this phenomenon.

## 1. THE EXPERIMENTAL SETUP AND METHOD

The experimental setup is shown in Fig. 1. Standard ruby laser 1 with a rotating-prism Q-switch was used. The energy per pulse was about 1 J, the pulse length was 40 nsec, and the typical beam divergence was 10′. Holder 2 for neutral filters and screens was placed next to the laser. Plane-parallel glass plates 3 served to divert a portion of the laser beam to first calorimeter 4, calibrated with reference to the laser beam energy, and to first photomultiplier 5 (FÉU-14). The first photomultiplier, a UR-4 amplifier, and an OK-21 oscilloscope were used to observe the laser pulse shape. The beam produced a spark in the focus of lens 6 (lenses with focal lengths from 4 to 10 cm were used). Solenoid 9 set up a magnetic field of 2200 Oe in the spark region parallel to the laser beam. The spark occurred inside measuring coil 8 connected to the OK-21 oscilloscope through amplifiers UR-3 and UR-4. To study slow processes, the OK-21 oscilloscope was replaced by an OK-17M type and the UR-4 amplifier was removed from the circuit.

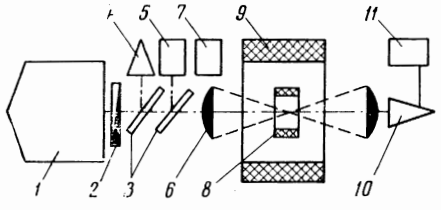


FIG. 1. Experimental setup. 1 — Q-switched laser; 2 — interchangeable filters; 3 — plane-parallel glass plates; 4 — first calorimeter; 5 — first photomultiplier; 6 — focusing lens; 7 — triggering photomultiplier; 8 — measuring coil; 9 — solenoid; 10 — second calorimeter; 11 — second photomultiplier.

After the laser beam passed through the spark, it was either picked up by second photomultiplier 11 and observed on the screen of the OK-21 oscilloscope, or allowed to enter the second calorimeter 10, which had an absolute calibration. The equipment included devices for the alignment and adjustment of the entire system and allowed for the displacement of individual components as desired.

The oscilloscopes recording the laser and induction signals were actuated by photomultiplier 7 sensing the light scattered by lens 6, and by the UR-4 amplifier. Owing to the finite actuation time of the oscilloscopes, the observed signals were sent through suitably matched long cables (of the RK-101 type); the cable length was 26 m for the OK-21 oscilloscope and 136 m for the OK-17M oscilloscope.

The magnetic-field perturbation was observed in terms of the emf induced in the measuring coil by the laser spark. The center of the coil was situated on the axis of the system and its plane was parallel to the axis. A 75 ohm resistor was connected across the input to the signal-carrying cable.

Two types of measuring coils were used. The first were low inductance coils of two turns, whose diameter varied from 0.46 to 3 cm. The time constant $\tau = L/R$ of the circuit was within the range of $(2 - 6) \times 10^{-9}$ sec. The signals R(t) of the low-inductance coils were proportional to $d\Phi/dt$, where $\Phi$ was the magnetic flux through the coil. High-

inductance integrating coils of many turns were also used. The integrating circuit consisted of the inductance of the measuring coil and the cable input resistor, and produced a signal that was proportional to $\Phi(t)$.

## 2. EXPERIMENTAL RESULTS

The longitudinal dimension of the region perturbing the field was determined by plotting (with the aid of the 0.71-cm diameter coil) the induction signal as a function of coil position on the z axis of the system. The plot is shown in Fig. 2. The same figure shows the corresponding theoretical function (normalized and aligned with the experimental curve with respect to the maximum) of field perturbation by a point dipole expressed by the well-known relation $\Delta\Phi = 2\pi M r_c^2/(z^2 + r_c^2)^{3/2}$, where M is the dipole magnetic moment and $r_c$ is the radius of the measuring coil. The comparison shows that the perturbation can be regarded with sufficient accuracy (of the order of 0.1 cm) as a point, and the center of the perturbation coincides with the lens focus.

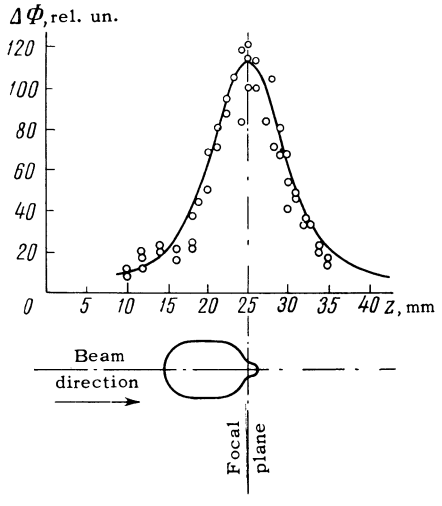


FIG. 2. Induction signal as a function of z. Below – outline of luminous spark region.

We know however that the visible size of the spark is fairly large. The same Fig. 2 shows an outline of the luminous regions of the spark drawn to a corresponding scale and obtained from time-integrated photographs of the spark. The luminous region appears to take up a considerable volume and extends towards the beam to a length of 12 mm, beginning with the focus of the lens.

In connection with the presence of the hot region of the spark, we note a small yet sharply outlined nipple-like projection in the near-focal area of the integrated spark photograph. It may possibly be due to the hot region of the spark.

The existence of the hot region was also confirmed by another type of experiment. As reported in[2], the laser spark is surrounded by a fairly large halo that is invisible against the bright glow of the spark but whose conductivity is detectable with the aid of microwave techniques and the ionization chamber (electric probe). The halo formation seems to be due mainly to the stepwise ionization by the ultraviolet emission from the spark.

We have prepared a miniature ionization chamber furnished with a system of collimating diaphragms (an "ionization telescope") to record ionization induced by radiation emitted from various regions of the spark. It was found that the most effective ionizing radiation was emitted by the near-focal region of the spark.

It is also possible to estimate the radial dimension of the spark (although the small longitudinal size is clearly due to the small radial dimension in this case). Assuming a point perturbation, it can be shown[3] that the emf induced in the measuring coil is inversely proportional to the coil radius. According to our experiments (Fig. 3), such a dependence does exist up to the radius of 0.23 cm. It follows then that the radial dimension of perturbation $r_0 \ll 0.23$ cm $= r_{max}$.

On the other hand, let us assume that the observed perturbation is due to a complete displacement of the external field from a region defined by the radius $r_{min}$ (the superconducting sphere approximation). We can then write $\frac{1}{2}Hr_{min}^3 = M$. Consequently, $r_{min} = (2M/H)^{1/3}$, and substituting the typical values of $10^{-2}$ Oe · cm$^3$ and $10^3$ Oe for M and H respectively, we have $r_{min} = 2.7 \times 10^{-2}$ cm. Hence $2.7 \times 10^{-2}$ cm $\ll r_0 \ll 2.3 \times 10^{-1}$ cm and owing to the strong inequalities on both sides we can assume an order of magnitude $r_0 \approx 8 \times 10^{-2}$ cm. Strictly speaking, however, the upper limit refers

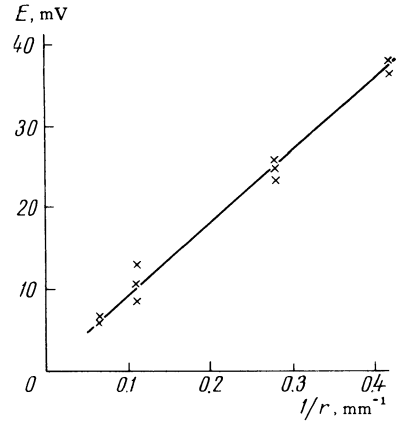


FIG. 3. Measuring coil emf as a function of coil radius.

only to the initial period of the perturbing region, and the plasma may possibly take up a larger volume in the course of subsequent expansion.

The minimal dimensions of the perturbing region can be compared with those of the near-focal region, which are determined by the well-known geometrical relations $z = f^2\varphi/d$ and $r = \frac{1}{4}f\varphi$, where z is the longitudinal dimension of the region, r is the radius of the region, f is the focal length of the lens, and d and $\varphi$ are the diameter and divergence of the beam respectively. Substituting typical experimental values, we have z = 1 mm and 2r = 0.1 mm.

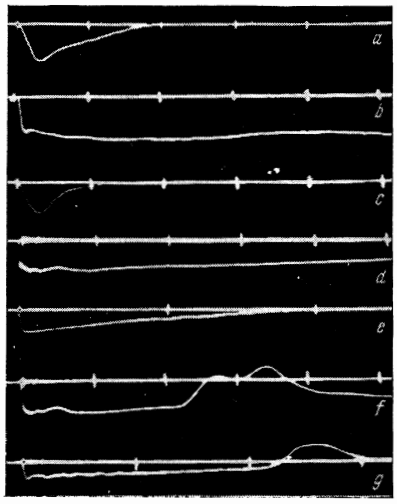


FIG. 4. Typical oscilloscope traces. a – M(t), 100 nsec per division; b – M(t), 100 nsec per division; c – laser emission intensity I(t), 100 nsec per division; d – M(t), 1 $\mu$sec per division, e – M(t), 20 $\mu$sec per division; f – M(t) with bushing, 1 $\mu$sec per division; g – M(t) with large diameter bushing, 2 $\mu$sec per division.

Figure 4 a shows a fast-sweep oscilloscope trace of the emf signal at the terminals of the low-inductance measuring coil, which is proportional to $\dot{M}$. Fig. 4b shows the emf signal at the terminal of the integrating coil, which is proportional to M. It can be seen that the rise time of the induction signal is fairly short (20—40 nsec) and approximately equal to the effective time of the laser beam (Fig. 4c). This seems to be due to the fact that the rapid motion of the plasma and its temperature rise stop when the laser beam is cut off (i.e., when the energy input to the spark ceases). We may note that the induction signal due to the displacement of the magnetic field does not change if a hollow dielectric cylinder ("bushing") with a sufficiently small internal radius (2 mm) is inserted into the measuring coil. This once again demonstrates that the factors responsible for the displacement of the field are localized in a small near-focal region. After the laser pulse has ceased there remains some slow rise in the magnetic moment and even some nonmonotonic components in the time dependence of the moment (Fig. 4d). This complex period of initial singularities in the life of the magnetic moment is apparently due to the inertial motion of the newly formed plasma and to the shock wave passing through the plasma, and lasts for 2—3 microsec.

This is followed by a slow monotonic disappearance of the magnetic moment, which is almost linear in time (slightly slower than linear). The characteristic lifetime is 30—40 $\mu$sec in this case (Fig. 4d).

The slow monotonic damping of the magnetic moment takes place, however, only if the radius of the integrating coil is sufficiently large (15—20 mm). If the spark region is surrounded by a hollow dielectric cylinder (bushing) with a small internal radius, then the slow decay of the perturbation changes at some instant t″ (Fig. 4f) into a relatively rapid decay (front $\approx 1$ $\mu$sec) followed by a complex nonmonotonic behavior of M(t) (Figs. 4f and 4g). The smaller the internal radius of the bushing the sooner the onset of the rapid decay of the perturbation.

Direct experiments with double probes placed on the internal surface of the bushing showed that the rapid perturbation decay is not due to the fact that the expanding plasma reaches eventually the bushing wall, where it undergoes cooling and reflection. The probes failed to detect the corresponding signals. However, the fact that the characteristic velocities $v = r/t''$ (where r is the bushing radius) are of the order of the sound velocity suggests that the sound wave (shock or ordinary) generated by the spark is a significant factor here.

Two functions were plotted to clarify this problem. The first was the lifetime of the slowly decaying perturbation as a function of bushing radius r. The second was the radius r as a function of time t′ required for the shock wave generated by the spark to travel the distance r. The latter dependence was obtained with the aid of the same measuring coil, into which we inserted (strictly coaxially, of course) tubes of various radii r made of thin metal foil. While this shielding eliminated the signal due to the spark perturbation of the field, the impact of the sound wave moved the tube, inducing a corresponding emf in the measuring coil. The above system represented thus an electrodynamic velocity pickup.

The functions under consideration are shown in Fig. 5. It shows that the spark gives rise to a shock

wave that in time becomes an ordinary sound wave propagating according to the linear law dr/dt = c. In the case given in Fig. 5, c = 430 m/sec, a velocity considerably exceeding that of sound at room temperature, 340 m/sec. Assuming $c \sim \sqrt{T}$, the air transmitting the sound pulse will have an effective temperature of 170°C. This is apparently connected with radiation heating of the ambient air by the spark and with the existence of the ionization halo.[2] A reduction in spark energy decreases the velocity of the sound pulse, which then approaches 340 m/sec on the linear segment of the r-t diagram.

It should be noted that the time t′ of impact of the sound wave against the dielectric bushing could not be discerned on either the M(t) or the M(t) plots.

Rapid decay of the spark begins approximately twice (1.8 times) as late, at the time t″. The rapid decay of the perturbation can be simply assumed as due to the return of the reflected sound wave to the axis of the system. The fact that the ratio of t″/t′ is somewhat less than two may be due to some air heating during the forward passage of the sound wave.

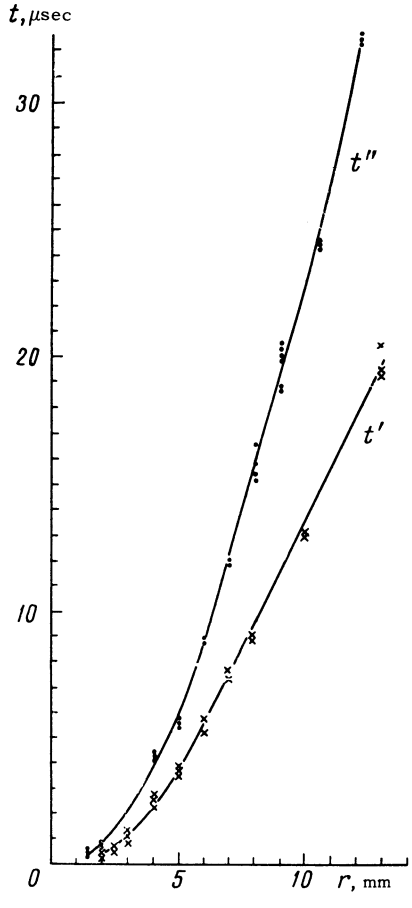


FIG. 5. Characteristic time values t′ and t″ as functions of radius.

The above experiments suggest the following mechanism of the phenomenon. The sufficiently conductive plasma created in the breakdown travels radially in the positive direction. The interaction of this motion with the longitudinal magnetic field gives rise to circular currents that cause a displacement of the field from the region of the spark, and we have a diamagnetic plasma. The sound pulse reflected from the bushing pulls the plasma towards the axis and this change in the velocity sign changes the direction of the circular currents; consequently, the magnetic flux through the near-axial region is increased, producing a kind of paramagnetic plasma. If the reversal of the magnetic moment has occurred early enough, the plasma has not been allowed to cool off, and its internal capability is high enough, further diffusive motion of the plasma away from the axis tends to restore the perturbation to some extent, or at least to restore its sign (Fig. 4f). On the other hand, if the perturbation sign reversal took place sufficiently late or the spark energy is low enough, the plasma formation will decay while remaining paramagnetic in nature (Fig. 4g). The actual phenomenon is more complicated, of course, and one should at least consider the long known fact[4] that the passage of a sound wave through a plasma sharply decreases its conductivity.

To determine the conductivity of the obtained plasma we use an expression taken from[3]

$$M = \frac{4\pi H}{3c^2}\int_0^R \sigma(r,t)\,v(r,t)\,r^3 dr,$$

and averaging yields

$$M_{av} = \frac{\pi H}{3c^2}\sigma_{av} v_{av} R^4.$$

Substituting typical values for $M = 10^{-2}$ Oe · cm$^3$ and $H = 10^3$ Oe, we have $\sigma_{av} v_{av} R^4 = 10^{16}$ cm$^5$/sec$^2$. Taking the sound velocity of $10^5$ cm/sec for $v_{av}$ (as expected from the experiments on the reversal of M) and $8 \times 10^{-2}$ cm for R (the average of $r_{min}$ and $r_{max}$ determined above), we have $\sigma_{av} = 2.6 \times 10^{15}$ sec$^{-1}$. This is a fairly large value for $\sigma$; it is not unreasonable, however, in view of the approximate nature of this estimate, and mainly because of the strong (fourth-power) dependence of the result on R. A change of R by less than a factor of two (by $10^{1/4} = 1.8$) changes the result by an order of magnitude.

In conclusion we note that diamagnetic (induction) signals similar to the above were also observed by us in a larger group of phenomena: in the course of focusing a laser beam on solid sur-

faces (giving rise to the so-called "flare") and when the beam is focused within transparent solids (leading to cracking of the near-focal region).

The authors thank M. S. Rabinovich for his interest in this work, G. A. Askar'yan for an evaluation, and L. M. Kolomiĭtsev for his assistance.

[1]G. A. Askar'yan, M. S. Rabinovich, M. M. Savchenko, and A. D. Smirnova, JETP Letters **1**, No. 1, 9 (1965), transl. p. 5.

[2]G. A. Askar'yan, M. S. Rabinovich, M. M. Savchenko, and A. D. Smirnova, JETP Letters **1**, No. 6, 18 (1965), transl. p. 162. G. A. Askar'yan, M. S. Rabinovich, M. M. Savchenko, and V. K. Stepanov, JETP Letters **3**, 465 (1966), transl. p. 303.

[3]G. A. Askar'yan and M. S. Rabinovich, JETP **48**, 290 (1965), Soviet Phys. JETP **21**, 190 (1965).

[4]C. G. Suits, Physics **6**, 190, 315 (1935).

Translated by J. G. Adashko
201